JACS
JOURNAL OF THE AMERICAN CHEMICAL SOCIETY
Article
pubs.acs.org/JACS

Stabilizing Catalytic Pathways via Redundancy: Selective Reduction of Microalgae Oil to Alkanes

Baoxiang Peng, Xiaoguo Yuan, Chen Zhao, and Johannes A. Lercher*

Department of Chemistry and Catalysis Research Center, Technische Universität München, Garching 85747, Germany

Supporting Information

ABSTRACT: A new route to convert crude microalgae oils using ZrO_2-promoted Ni catalysts into diesel-range alkanes in a cascade reaction is presented. Ni nanoparticles catalyze the selective cleavage of the C−O of fatty acid esters, leading to the hydrogenolysis of triglycerides. Hydrogenation of the resulting fatty acids to aldehydes (rate-determining step) is uniquely catalyzed via two parallel pathways, one via aldehyde formation on metallic Ni and the second via a synergistic action by Ni and ZrO_2 through adsorbing the carboxylic groups at the oxygen vacancies of ZrO_2 to form carboxylates and subsequently abstracting the α-hydrogen atom to produce ketene, which is in turn hydrogenated to aldehydes and decarbonylated on Ni nanoparticles.

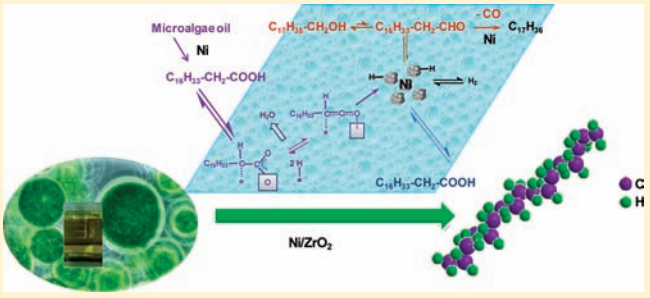

INTRODUCTION

Ready-to-use diesel range components instead of biodiesel (fatty acid alkyl esters) produced from triglycerides are considered one of the most promising energy carriers derived from renewable energy sources.[1,2] Microalgae is a highly potential raw material for the triglyceride feedstock, not only because of its high oil content (up to 60 wt %)[3,4] and the rapid growth rate of algae,[5−7] but also because its cultivation does not compete with edible food or oil production for arable land.

Two catalytic hydrodeoxygenation approaches have been reported for the transformation of crude microalgae oil to diesel-range alkanes. One option employs sulfide-based catalysts, such as Ni- and Co-promoted molybdenum sulfides in hydrotreating-like processes.[8,9] However, the sulfide catalysts lead to contamination of the alkane products by organosulfur compounds and deactivate via sulfur leaching, especially in the presence of ubiquitous traces of water.[10,11] The second approach relies on novel sulfur-free zeolite-supported Ni catalysts, such as Ni/H-β, to produce C_{15}−C_{18} alkanes via hydrodeoxygenation.[12] Considering that the hydrogen consumption for deoxygenation of triglycerides decreases from hydrodeoxygenation via decarbonylation to decarboxylation,[13] the latter two routes (decarbonylation and decarboxylation) would be conceptually more cost- and energy-efficient than the hydrodeoxygenation route.

Stimulated by reports of the selective reduction of carboxylic acids by slightly reducible oxides,[14,15] we have explored combinations of such oxide supports with base metals that catalyze reductive decarbonylation and decarboxylation. Here, we report that Ni nanoparticles together with ZrO_2 can selectively cleave C−C bonds for converting C_{18} stearic acid to C_{17} *n*-heptadecane in uniquely stable, redundant mono- and dual-functional routes catalyzing the tandem hydrogenation−decarbonylation of the fatty acid. We also demonstrate that this approach converts crude microalgae oils efficiently into sulfur-free alkanes using ZrO_2 catalysts combining high reactivity and stability in both batch and continuous flow mode at relatively milder conditions (270 °C, in the presence of 40 bar H_2).

RESULTS AND DISCUSSION

Catalyst Screening. Initially, five oxide supports were selected to disperse the Ni nanoparticles using incipient wetness impregnation. The physicochemical properties of the resulting materials and the techniques to evaluate these catalysts are summarized in the Supporting Information (see Table S1). The average Ni particle sizes of Ni/ZrO_2 increased from 5 to 18 nm (determined by XRD) as the Ni content increased from 3 to 15 wt %, whereas the Ni particle sizes varied between 10 and 20 nm for other oxide supports (Ni loading: 10 wt %). The specific surface areas of ZrO_2-, TiO_2-, CeO_2-, Al_2O_3-, and SiO_2-supported Ni catalysts (10 wt %) were 100, 50, 95, 80, and 170 m^2/g, respectively. The acid and base site concentrations of the parent ZrO_2 were 0.103 and 0.169 mmol/g, respectively, both of which gradually decreased as the Ni content increased (see Table S1, Supporting Information [SI]).

To explore the impact of support, the catalytic conversion of stearic acid was carried out at 260 °C with 40 bar H_2 in batch mode on samples with different supports (see Table 1). *n*-Heptadecane was obtained almost quantitatively with all Ni/ZrO_2 catalysts with initial rates of 1.2−2.5 $mmol \cdot g^{-1} \cdot h^{-1}$. At the lowest Ni content (3 wt %), the yield of C_{17} *n*-heptadecane was 51%, with 33% C_{18} 1-octadecanol and 7% stearyl stearate

Received: March 12, 2012
Published: April 30, 2012

   dx.doi.org/10.1021/ja302436q | J. Am. Chem. Soc. 2012, 134, 9400−9405

Table 1. Comparison of Stearic Acid Conversion over Different Catalysts at 260 °C[a]

catalyst	rate[b] (mmol·g^{-1}·h^{-1})	conv. (%)	selectivity (C%) n-C_{17}	n-C_{18}	A[c]	C[c]	E[c]
ZrO_2[d]	0.07	13	3.2	–	29	–	12
3 wt % Ni/ZrO_2	1.2	96	51	2.5	33	3.4	7.6
5 wt % Ni/ZrO_2	1.9	100	90	2.0	6.7	1.0	–
10 wt % Ni/ZrO_2	2.2	100	96	1.5	1.2	1.2	–
15 wt % Ni/ZrO_2	2.5	100	96	1.5	1.4	1.3	–
10 wt % Ni/TiO_2	2.1	98	87	5.0	6.7	0.9	0.7
10 wt % Ni/CeO_2	2.0	100	93	0.4	3.5	2.8	–
10 wt % Ni/Al_2O_3	1.0	63	81	0.7	14	0.9	3.5
10 wt % Ni/SiO_2	0.6	45	57	1.5	34	1.3	5.8

[a]Reaction conditions: stearic acid (1.0 g), dodecane (100 mL), catalyst (0.5 g), 40 bar H_2, 8 h. [b]Initial hydrogenation rate. [c]**A** = 1-octadecanol, **C** = cracking, **E** = stearyl stearate. [d]56% selectivity: stearone obtained from ketonization of stearic acid.

produced. The pure ZrO_2 support led to selectivities of 3.2% C_{17} alkane, 29% C_{18} 1-octadecanol, 56% C_{31} stearone, and 12% C_{32} stearyl stearate at 13% conversion, showing an initial hydrogenation rate of 0.07 mmol·g^{-1}·h^{-1}. Stearone was produced by the ketonization of stearic acid, and stearyl stearate was formed via esterification of stearic acid with 1-octadecanol intermediate on acid–base sites. By comparison, Ni/TiO_2 and Ni/CeO_2 (10 wt %) showed quantitative conversion under these conditions with initial rates of ~2.0 mmol·g^{-1}·h^{-1} but led to slightly lower selectivities to C_{17} n-heptadecane at 87% and 93%, respectively. Ni/Al_2O_3 and Ni/SiO_2 were less active and selective; they gave 45–63% conversions and n-heptadecane selectivities of 81%, and 57%, respectively.

Kinetics of Stearic Acid and 1-Octadecanol Conversion. The mechanism of stearic acid deoxygenation was explored with 10 wt % Ni/ZrO_2 (see Figure 1). The yield of C_{17} n-heptadecane continuously increased to 96% for 8 h with increasing conversion, while that of 1-octadecanol increased gradually to 28% and then decreased at higher conversions. Only traces of octadecanal (<0.2 C %) were detected.

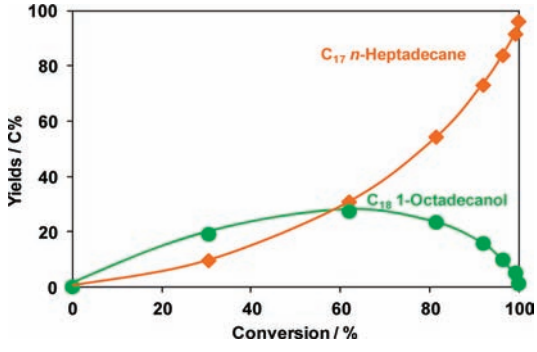

Figure 1. Yields of n-heptadecane and 1-octadecanaol as a function of stearic acid conversion over 10 wt % Ni/ZrO_2. The conversion and yield data were sequentially recorded at 0, 60, 120, 180, 240, 300, 360, 480 min. Reaction conditions: stearic acid (1.0 g), dodecane (100 mL), 10 wt % Ni/ZrO_2 (0.5 g), 40 bar H_2.

The intermediate 1-octadecanol was converted in a separate experiment on 10 wt % Ni/ZrO_2 at conditions identical to stearic acid conversion in order to explore the catalytic chemistry of the deoxygenation of aliphatic alcohols (see Figure 2A). The yield of n-heptadecane increased almost

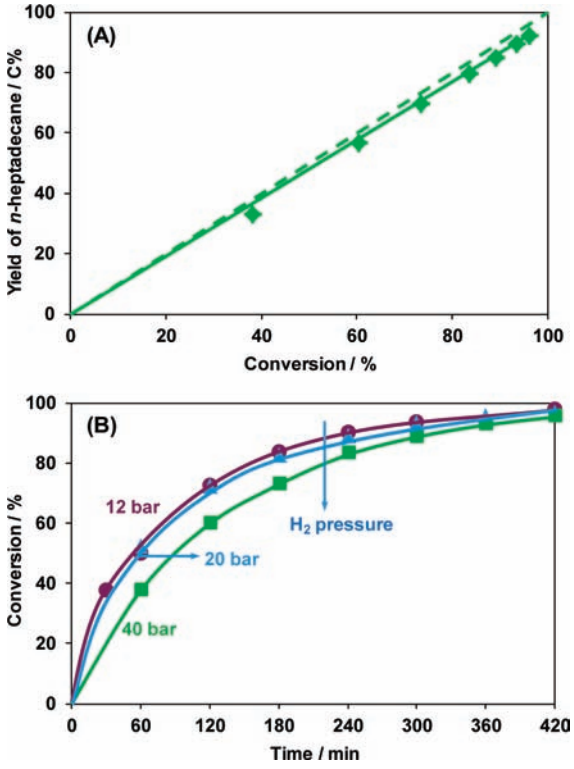

Figure 2. (A) Yield of C_{17} n-heptadecane versus C_{18} 1-octadecanol conversion. The conversion and yield data were sequentially recorded at 0, 60, 120, 180, 240, 300, 360, 420 min. (B) Impact of H_2 pressure on C_{18} 1-octadecanol conversion as a function of time. Reaction conditions: 1-octadecanol (1.0 g), 10 wt % Ni/ZrO_2 (0.15 g), dodecane (100 mL), 260 °C, stirred at 600 rpm; (A) 40 bar H_2; (B) 12, 20, 40 bar H_2.

linearly with 1-octadecanol conversion, attaining 92% n-heptadecane yields after 7 h together with 3% yields of C_{18} alkane which was formed via a tandem dehydration–hydrogenation route. This implies that the equilibrium between the alcohol and the aldehyde was achieved from which the decarbonylation of 1-octadecanol to n-heptadecane took place.

Hydrogenation–dehydrogenation thermodynamic data (see Figure S2 [SI]) show that 1-octadecanol/octadecanal ratios increase with H_2 pressure. Note that the equilibrium constant K ($a_{alcohol}/(a_{aldehyde}\cdot a_{H2})$) is approximately 57 at 260 °C in presence of 40 bar H_2 with a denoting the activity of the reacting components. The equilibration is consistent with the observed trace concentrations of octadecanal during the conversion of stearic acid and 1-octadecanol. The reaction rate increased dramatically as the H_2 partial pressure decreased from 40 to 12 bar (see Figure 2B). The initial decarbonylation rate of 1-octadecanol at 12 bar H_2 (16.0 mmol·g^{-1}·h^{-1}) was 2-fold larger than that at 40 bar H_2, reflecting that the higher equilibrium octadecanal concentrations (from eliminating 1 mol of H_2 from 1-octadecanol) led to higher decarbonylation

dx.doi.org/10.1021/ja302436q | J. Am. Chem. Soc. 2012, 134, 9400–9405

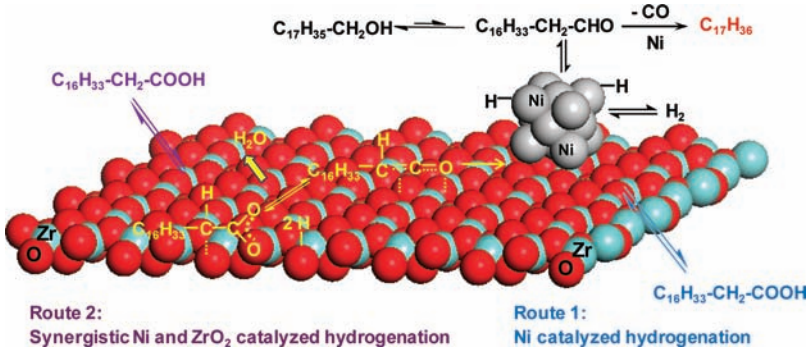

Figure 3. Proposed reaction mechanism for deoxygenation of stearic acid to C_{17} *n*-heptadecane via synergistic catalysis over Ni/ZrO_2.

Table 2. Fatty Acid Composition of Microalgae Oil [a]

fatty acids composition [wt %]												
$C_{14:0}$ [b]	$C_{16:0}$	$C_{18:2}$	$C_{18:1}$	$C_{18:0}$	$C_{20:4}$	$C_{20:0}$	$C_{22:6}$	$C_{22:4}$	$C_{22:1}$	$C_{22:0}$	$C_{24:0}$	sterol
0.04	4.41	56.2	32.2	4.41	0.07	0.43	0.13	0.19	0.97	0.44	0.36	0.12

[a]Crude microalgae oil provided by Verfahrenstechnik Schwedt GmbH. [b]The nomenclature shows the number of carbon atoms and the number of C═C double bonds: for example the alkyl chain of the present fatty acid contains 14 C atoms and no double bonds.

rates. Note that the catalytic decarbonylation routes closely resemble those of C_3 alcohols on Pt/Al_2O_3 catalysts.[16,17]

The individual kinetics of stearic acid and 1-octadecanol show that decarbonylation rates (8.1 $mmol \cdot g^{-1} \cdot h^{-1}$) are approximately 4 times higher than the hydrogenation rate of stearic acid (2.2 $mmol \cdot g^{-1} \cdot h^{-1}$). Thus, the hydrogenation step is concluded to have the slowest forward rate constant in the overall reaction. The apparent activation energy of 151 kJ/mol for stearic acid hydrogenation is quite high, which is in line with the slowest reaction rate (see Figure S3 [SI]). On the basis of the above results and analysis, we conclude that the main reaction route for stearic acid conversion on Ni/ZrO_2 proceeds via acid hydrogenation (rate-determining step) to form the aldehyde (in equilibrium with the corresponding alcohol), which is in turn rapidly decarbonylated to heptadecane on Ni by eliminating CO.

Mechanism into the Deoxygenation of Stearic Acid to C_{17} *n*-Heptadecane via Synergistic Catalysis over Ni/ZrO_2. The turnover frenquencies (TOF, mol of reactant converted per mole of accessible Ni within a chosen time) for hydrogenation of stearic acid attained were approximately 12 h^{-1} over Ni/ZrO_2, Ni/TiO_2, and Ni/CeO_2 catalysts, which were 2 times higher than those over Ni/Al_2O_3 and Ni/SiO_2 catalysts (see Figure S4, SI). It clearly demonstrates that Ni is able to efficiently catalyze the hydrogenation of stearic acid to octadecanal (Route 1, Figure 3). The higher activity with reducible supports, however, also shows that the support plays an important role in the reductive conversion of stearic acid to octadecanal (rate-determining step). The fact that pure ZrO_2 exhibited some activity for stearic acid reduction (see Table 1) indicates that it is able to provide a parallel reaction pathway to octadecanal, in addition to the reduction at the Ni surface. The reducible oxides of ZrO_2, TiO_2, and CeO_2 selectively hydrogenate carboxylic acids to aldehydes by concerted adsorption of the acid at oxygen vacancies of metal oxides to form carboxylates and dihydrogen activation via dissociative adsorption on oxygen defect sites of the ZrO_2 surface[14,15,18] (see Route 2 at Figure 3). The α-hydrogen atoms of the carboxylate can be subsequently abstracted to produce a ketene intermediate,[19] which is further hydrogenated to octadecanal on Ni nanoparticles. The remaining two protons including one generated in the adsorption of the stearic acid and the other formed from the abstraction of α-hydrogen atom of the alkyl chain, recombine with the oxygen bound at the ZrO_2 defect site and desorb as molecular water. Thus, we conclude that stearic acid is reduced to octadecanal via two parallel routes, one catalyzed by Ni nanoparticles and the other catalyzed synergistically by Ni and ZrO_2. These dual routes create a redundancy in the surface reaction that is only found in enzyme catalysis. Whatever the route of generation, octadecanal is in turn decarbonylated to *n*-heptadecane on the Ni nanoparticles (see Figure 3).

Deoxygenation of Microalgae Oil with Ni/ZrO_2 Catalysts in Batch and Continuous Flow Reactor. Having identified Ni/ZrO_2 as an excellent catalyst to reduce stearic acid to the corresponding alkane allows us to convert crude microalgae oil that mainly consists of neutral lipids such as mono-, di-, and triglycerides. The fatty acid composition of microalgae oil used for this work comprises unsaturated C_{18} fatty acids (88.4 wt %), saturated C_{18} fatty acids (4.4 wt %), as well as some other C_{14}, C_{16}, C_{20}, C_{22}, and C_{24} fatty acids (7.1 wt % in total) (see Table 2).

It demonstrated that 68 wt % yield of *n*-heptadecane and 76 wt % yield of total liquid alkanes were attained at 270 °C after 8 h (see Figure 4), and the latter value was very close to the theoretical yield (81 wt %).[20] The yields of stearic acid (primary intermediate) and 1-octadecanol (secondary intermediate) both increased at first to a maximum value (18 wt % and 8 wt %, respectively) and then decreased to zero as the reaction was completed. Propane (3.6 wt %) and methane (4.6 wt %) were the main products in the vapor phase, which were formed by the hydrogenolysis of triglyceride and the methanation of CO/CO_2 with H_2, respectively. The final carbon distributed in the liquid phase as C_{17} *n*-heptadecane (major) and other $C_{13}-C_{21}$ hydrocarbons (minor), and in the gas phase as propane and methane.

To investigate the stability of the catalyst, this process was transferred to continuous flow operation, in which the crude microalgae oil was hydrotreated with Ni/ZrO_2 catalysts in a trickle bed reactor at identical conditions (270 °C, 40 bar H_2)

dx.doi.org/10.1021/ja302436q | J. Am. Chem. Soc. 2012, 134, 9400−9405

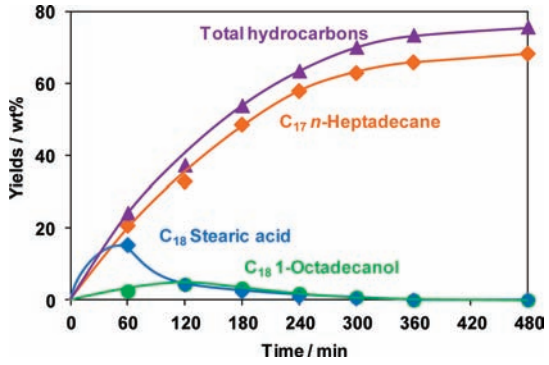

Figure 4. Product distributions for the transformation of microalgae oil over 10 wt % Ni/ZrO_2 as a function of time. Reaction conditions: microalgae oil (1.0 g), 10 wt % Ni/ZrO_2 (0.5 g), 270 °C, 40 bar H_2, stirred at 600 rpm.

(see SI for detailed procedures). It led to 70 wt % yield of C_{17} *n*-heptadecane and 75 wt % yield of total liquid alkanes, which was almost identical to the results obtained in the batch reactor. Note that the catalysts did not deactivate after 72 h (see Figure S6, SI), demonstrating its high stability.

Combining the overall kinetics of microalgae oil conversion with the knowledge from the deoxygenation of stearic acid and 1-octadecanol, the main reaction pathways for the transformation of microalgae oil with Ni/ZrO_2 (see Scheme 1) is

Scheme 1. Proposed Main Reaction Pathways for Microalgae Oil Transformation to Alkanes over Ni/ZrO_2 Catalyst

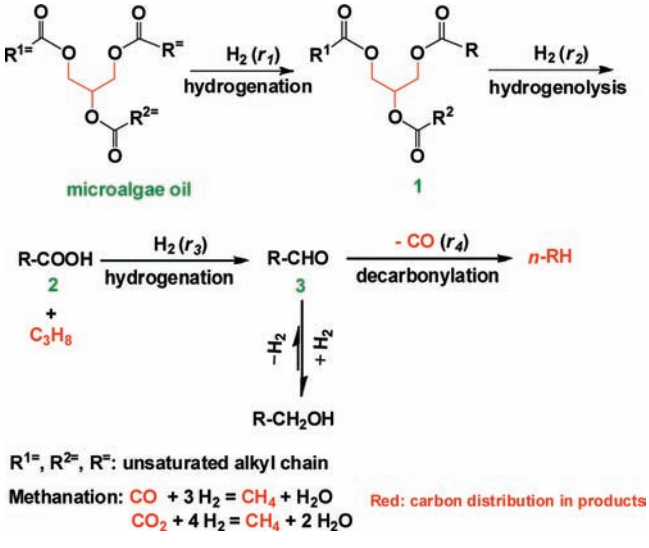

concluded to proceed via initial hydrogenation of the C=C double bonds in the alkyl chain, followed by selective cleavage of the C−O bond of the formed saturated triglyceride to fatty acids and propane via hydrogenolysis. The subsequent hydrogenation of the carboxylic group of the fatty acid leads to the corresponding aldehyde (rate-determining step) either catalyzed solely by metallic Ni or synergistically by Ni and ZrO_2 via a ketene as intermediate, followed by the decarbonylation of octadecanal to the target *n*-heptadecane and carbon monoxide (C−C bond cleavage, major route). It can also be deduced that the individual reaction rates follow the order of r_1 (hydrogenation of C=C double bonds in the alkyl chain) ≫ r_2 (hydrogenolysis of saturated triglyceride) > r_4 (decarbonylation of alcohol) > r_3 (hydrogenation of fatty acid, rate-determining step). In addition, the hydrodeoxygenation and decarboxylation of stearic acid lead to C_{18} *n*-octadecane and C_{17} *n*-heptadecane (minor routes), respectively. The weak acid sites of ZrO_2 catalyze slight cracking and isomerization of the produced alkanes, albeit with low rates. CO and CO_2 may react with H_2 to produce methane and water, which could be eventually recycled by reforming or be used as heating fuels.

With increasing H_2 pressure from 6 to 40 bar (see Figure 5), the yield of *n*-heptadecane increased remarkably from 26 to 66

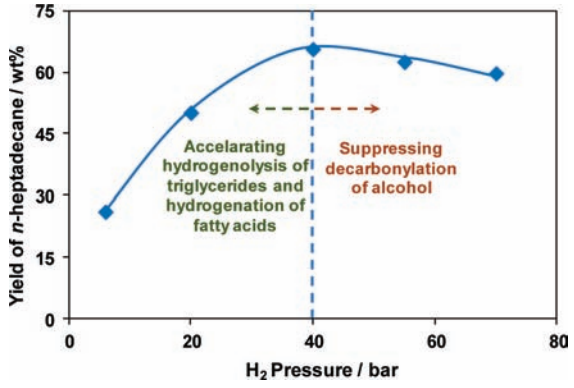

Figure 5. Impact of H_2 pressure on the yield of *n*-heptadecane for microalgae oil conversion. Reaction conditions: microalgae oil (1.0 g), dodecane (100 mL), 10 wt % Ni/ZrO_2 (0.5 g), 260 °C, 8 h, stirred at 600 rpm.

wt %, which is attributed to the greatly enhanced tandem hydrogenation reaction rates of r_1, r_2, and r_3. However, further increase of the H_2 pressure from 40 to 70 bar led to a slight decrease of the *n*-heptadecane yield from 66 to 59 wt %, as the decarbonylation rate r_4 is suppressed at high H_2 pressure, when the equilibrium shifts from octadecanal to 1-octadecanol.

CONCLUSION

In summary, a novel route for the transformation of microalgae oil to alkanes has been developed by selectively cleaving C−C and C−O bonds with ZrO_2-supported Ni catalysts. The hydrogenolysis of triglyceride, the decarbonylation of aldehyde, and the hydrogenation of functional groups (that is, −COOH, −CHO, C=C) are catalyzed by metallic Ni. The rate-determining hydrogenation of the fatty acid is either catalyzed solely by metallic Ni to form aldehyde or catalyzed by synergistic Ni and the ZrO_2 support through adsorbing the carboxylic group at the oxygen vacancy of ZrO_2 to form carboxylate and abstracting α-hydrogen atoms to produce the ketene intermediate, which can be in turn hydrogenated to aldehydes over the Ni particles. The hydrogenolysis/hydrogenation−decarbonylation route is shown to be feasible and superior to the hydrodeoxygenation pathway due to the lower hydrogen consumption. This approach holds great potential for producing sulfur-free green transportation fuels from microalgae oil at large scale.

EXPERIMENTAL SECTION

Chemicals. All chemicals were obtained from commercial suppliers: stearic acid (Fluka, analytical standard), 1-octadecanol (Fluka, ≥99.5% GC assay), dodecane (Sigma-Aldrich, ≥99% Reagent Plus), eicosane (Aldrich, ≥99% GC assay), *n*-octadecane (Fluka, ≥99% GC assay), *n*-heptadecane (Fluka, ≥99% GC assay), nickel(II) nitrate hexahydrate (Sigma-Aldrich, ≥98.5%), ZrO_2 (MEL Chem-

dx.doi.org/10.1021/ja302436q | J. Am. Chem. Soc. 2012, 134, 9400−9405

icals), TiO_2 (Degussa P25), CeO_2 (Rhodia HAS-10), SiO_2 (Aeroxide Alu C-Degussa), and Al_2O_3 (Aeroxide Alu C-Degussa). Microalgae oil was provided by Verfahrenstechnik Schwedt GmbH.

Catalyst Preparation. Ni supported on ZrO_2, TiO_2, CeO_2, SiO_2, and Al_2O_3 were synthesized by the wetness impregnation method. The ZrO_2 support was prepared from zirconium hydroxide by calcination in air at 400 °C for 4 h. For example, the procedure for preparing 10 wt % Ni/ZrO_2 follows: $Ni(NO_3)_2{\cdot}6H_2O$ (5.83 g) was dissolved in water (10 g), and then such solution was slowly dropped onto ZrO_2 (10 g) with continuous stirring. After metal incorporation with support at ambient temperature for 4 h, the catalyst was first dried overnight at ambient temperature and then dried at 110 °C for 12 h. Afterward, the catalyst was calcined in synthetic air at 400 °C for 4 h (flow rate = 100 mL/min) and reduced at 500 °C for 4 h (ramp = 2 °C/min) in hydrogen (flow rate = 100 mL/min).

Catalyst Characterization. *Atomic Absorption Spectroscopy (AAS).* The metal loading was determined by atomic absorption spectroscopy using a UNICAM 939 AA-spectrometer. Prior to measurement, the sample was dissolved in a mixture of hydrofluoric acid (48%) and nitro-hydrochloric acid at the boiling point of the mixture (about 110 °C).

BET Specific Surface Area. The BET specific surface area was determined by nitrogen adsorption−desorption at −196 °C using the Sorptomatic 1990 series instrument. The sample was activated in vacuum at 300 °C for 2 h before measurement.

Temperature-Programmed Desorption (TPD). Temperature-programmed desorption of ammonia or carbon dioxide was performed in a 6-fold parallel reactor system. The catalysts were activated in He at 500 °C (5 °C/min ramp) for 1 h. NH_3 and CO_2 were adsorbed with partial pressures of 1 mbar at 100 or 35 °C, respectively. Subsequently, the samples were purged with 30 mL/min He for 2 h in order to remove physisorbed molecules. For the temperature-programmed desorption experiments, six samples were sequentially heated from 100 to 765 °C with an increment of 10 °C/min to desorb ammonia and from 35 to 450 °C to desorb carbon dioxide. The rates of desorbing species were monitored by mass spectrometry (Balzers QME 200). For the quantification of amount of acidity, a standard HZSM-5 zeolite (Si/Al = 45) with known acid site concentration was used to calibrate the signal. The response of the CO_2 signal was calibrated using the decomposition of $NaHCO_3$.

X-ray Powder Diffraction (XRD). The structures of the metal oxides-supported Ni catalysts were analyzed by X-ray diffraction using a Philips X'Pert Pro System. The radiation source was Cu Kα operating at 40 kV/45 mA. The sample was measured with a scan rate of 1 deg/min from 5° to 70° (2θ). The metal particle size was calculated from diffraction by te Scherrer equation. The XRD patterns of the prepared Ni-based catalysts are displayed in Figure S1 [SI].

Experimental Procedure for Reaction in the Autoclave. The typical experiments with microalgae oil, stearic acid, or 1-octadecanol were carried out as follows: reactant (1.0 g), dodecane (100 mL), and catalyst (0.5 g) were loaded into the batch autoclave (Parr Instrument, 300 mL). Then the autoclave was purged with N_2 at ambient temperature, and until the required temperature was achieved, it was pressurized by H_2. The reaction was carried out at 260 °C in presence of 40 bar H_2 (reaction temperature) at a stirring speed of 600 rpm for 8 h. The products in the vapor phase were analyzed by the online gas chromatograph (GC), while the liquid samples were manually collected during the run and later analyzed by GC−MS.

Conversion = (weight of converted reactant/weight of the starting reactant) × 100%. Yield (C%) = (C atoms in each product/C atoms in the starting reactant) × 100%. Yield (wt %) = (weight of each product/weight of the starting reactant) × 100%.

Experimental Procedure for Reaction in the Continuous Flow Reactor. The continuous flow reaction system with a trickle bed reactor used for the catalyst stability and deactivation test is schematically shown in Figure S4 [SI]. The stainless steel tubular reactor (1/4 in. o.d.) was loaded with 0.5 g catalyst with a particle size between 150 and 280 μm. After the reduction of the catalysts in H_2 at 450 °C for 2 h, the system was kept at 270 °C and pressurized with H_2 to 40 bar. A liquid solution of microalgae oil in dodecane (1.33 wt %, 0.2 mL/min) was introduced into the system with the HPLC pump. The liquid samples were separated from the effluents by the 16-port sampling loop, collected in 16 vials, and finally analyzed by GC−MS.

Analysis Method. Liquid products were analyzed by a Shimadzu 2010 GC−MS equipped with a HP-5 capillary column (30 m, 0.32 mm inner diameter, 0.25 μm film). Internal standard (i.e., eicosane) was used for quantification. Both injection and detection temperatures are 320 °C. The temperature program is set in the following way: from 60 to 80 °C (rate: 2 °C/min), then increase to 300 °C (rate: 10 °C/min) and hold for 15 min. Note that by using a high injection port temperature, e.g., 320 °C, reliable and direct quantification for fatty acids can be achieved without chemical derivitization. The vapor phase was analyzed online by a gas chromatograph with TCD detector and two capillary columns (MS-5A and HP-Plot Q).

■ ASSOCIATED CONTENT

Supporting Information

Catalyst characterization, impact of reaction temperature on stearic acid conversion, turnover frequency (TOF) for stearic acid conversion with different catalysts, microalgae oil conversion in the continuous flow reactor. This material is available free of charge via the Internet at http://pubs.acs.org.

■ AUTHOR INFORMATION

Corresponding Author

johannes.lercher@ch.tum.de

Notes

The authors declare no competing financial interest.

■ ACKNOWLEDGMENTS

We appreciate the partial financial support from EADS Deutschland GmbH. The work is also partially supported by Technische Universität München in the framework of European Graduate School for Sustainable Energy.

■ REFERENCES

(1) Kubicka, D.; Horacek, J. *Appl. Catal., A* **2011**, *394*, 9.
(2) Li, L. X.; Coppola, E.; Rine, J.; Miller, J. L.; Walker, D. *Energy Fuels* **2010**, *24*, 1305.
(3) Mata, T. M.; Martins, A. A.; Caetano, N. S. *Renewable Sustainable Energy Rev.* **2010**, *14*, 217.
(4) Schenk, P. M.; Thomas-Hall, S. R.; Stephens, E.; Marx, U. C.; Mussgnug, J. H.; Posten, C.; Kruse, O.; Hankamer, B. *Bioenergy Res.* **2008**, *1*, 20.
(5) Wijffels, R. H.; Barbosa, M. J. *Science* **2010**, *329*, 796.
(6) Chisti, Y. *Biotechnol. Adv.* **2007**, *25*, 294.
(7) Huber, G. W.; Iborra, S.; Corma, A. *Chem. Rev.* **2006**, *106*, 4044.
(8) Sotelo-Boyás, R.; Liu, Y. Y.; Minowa, T. *Ind. Eng. Chem. Res.* **2011**, *50*, 2791.
(9) Huber, G. W.; O'Connor, P.; Corma, A. *Appl. Catal., A* **2007**, *329*, 120.
(10) Viljava, T. R.; Komulanien, R. S.; Krause, A. O. I. *Catal. Today* **2000**, *60*, 83.
(11) Laurent, E.; Delmon, B. *J. Catal.* **1994**, *146*, 281.
(12) Peng, B.; Yao, Y.; Zhao, C.; Lercher, J. A. *Angew. Chem., Int. Ed.* **2012**, *51*, 2072.
(13) The equations below display the hydrodeoxygenation, decarbonylation, and decarboxylation pathways for alkane production using fatty acid as reactant. As fatty acid can be used as a representative reactant, similar equations can be written for triglycerides conversion.

$$\text{Hydrodeoxygenation: } R{-}COOH + 3H_2 \rightarrow R{-}CH_3 + 2H_2O \quad (1)$$

$$\text{Decarbonylation: } R{-}COOH + H_2 \rightarrow R{-}H + CO + H_2O \quad (2)$$

Decarboxylation: $R-COOH \rightarrow R-H + CO_2$ (3)

(14) Yokoyama, T.; Yamagata, N. *Appl. Catal., A* **2001**, *221*, 227.
(15) Yokoyama, T.; Setoyama, T.; Fujita, N.; Nakajima, M.; Maki, T. *Appl. Catal., A* **1992**, *88*, 149.
(16) Wawrzetz, A.; Peng, B.; Hrabar, A.; Jentys, A.; Lemonidou, A. A.; Lercher, J. A. *J. Catal.* **2010**, *269*, 411.
(17) Peng, B.; Zhao, C.; Mejía-Centeno, I.; Fuentes, G. A.; Jentys, A.; Lercher, J. A. *Catal. Today* **2012**, *183*, 3.
(18) Pestman, R.; Koster, R. M.; Boellaad, E.; Van der Kraan, A. M.; Ponec, V. *J. Catal.* **1998**, *174*, 142.
(19) Pestman, R.; Koster, R. M.; Pieterse, J. A. Z.; Ponec, V. *J. Catal.* **1997**, *168*, 265.
(20) The theoretical yield of liquid alkanes from microalgae oil is 81 wt % based on the decarbonylation pathway. The theoretical yields for propane and methane are 4.6 wt % and 5.3 wt %, respectively.